J. Synchrotron Rad. (1995). 2, 31–35

# Polarized Dispersion for X-rays Scattered by an Aromatic Bromide

**Lieselotte K. Templeton and David H. Templeton**

*Department of Chemistry, University of California, Berkeley, CA 94720, USA*

*(Received 28 March 1994; accepted 24 August 1994)*

Second-rank tensors describing how the real and imaginary dispersion terms $f'$ and $f''$ depend on photon polarization for Br atoms substituted on a benzene ring have been measured at six energies near the Br $K$ absorption edge in diffraction experiments with synchrotron radiation and crystals of homocubanecarboxylic acid $p$-bromoanilide. Resonance with a $\sigma$ antibonding orbital causes $f'$ to change with polarization as much as 4.3 and $f''$ as much as 7.5. The tensors for two independent Br atoms are equal, uniaxial and aligned with the respective Br–C bond. Absorption spectra show the average effect of two tensors with different orientations. Atomic coordinates from a new refinement of the structure are listed.

**Keywords: anisotropic anomalous scattering; X-ray dichroism; homocubane.**

## 1. Introduction

The dispersion of optical properties for X-rays with wavelengths near absorption edges involves electronic transitions from core levels to states within or just above the valence shell. When these excited states lack high symmetry and are oriented in space, as in a molecule in a crystal, the atomic scattering factor can exhibit anisotropy with respect to photon polarization that sometimes amounts to many electron units per atom (Templeton & Templeton, 1985*b*). This anisotropy provides some new ways to find phases of structure factors (Templeton & Templeton, 1987, 1991, 1992; Kirfel & Petcov, 1991, 1992). It can also be a complication that needs attention in the multiwavelength anomalous diffraction (MAD) method of phase determination (Fanchon & Hendrickson, 1990).

Bromine is a good element to use in the MAD method because its $K$ edge is at a convenient wavelength (0.92 Å) and because it can be incorporated in a macromolecule at definite positions, for example substituted for hydrogen on aromatic rings (Hendrickson, 1991). It exhibits a variety of resonance effects at the $K$ edge, with pronounced dichroism in two cases where it is bonded covalently: $Br_2$ (Heald & Stern, 1978) and $BrO_3^-$ (Templeton & Templeton, 1985*a*). We expected that dichroism much like that found in $Br_2$ would occur in Br bonded to carbon because in each case Br has a single covalent bond. Here we report a study of an aromatic bromide that verifies this prediction and also provides data which may be helpful in the use of such compounds in diffraction experiments. This experiment used linearly polarized X-rays at the Stanford Synchrotron Radiation Laboratory (SSRL).

In a search for a compound suitable for this work we found crystals of homocubanecarboxylic acid $p$-bromoanilide (1) that had been prepared by Dauben & Whalen (1966) for a crystallographic verification of the topology of the homocubane cage. The structure was determined by Pettersen (1966) using intensity data measured at fixed angle with a manual diffractometer ($R = 0.060$ for 2252 reflections). The symmetry and molecular orientations permit duplicate measurements of the atomic scattering tensor of Br from diffraction data. The X-ray absorption spectra also reveal the optical anisotropy, but with some ambiguity with regard to the atomic tensors. We repeated the structure determination to get more accurate parameters for use in the calculation of the tensors.

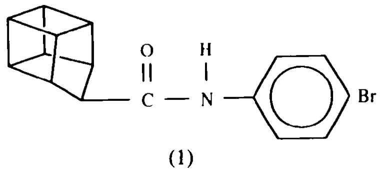

(1)

## 2. Crystal structure

$N$-(4-Bromophenyl)pentacyclo[4.3.0.0$^{2,5}$.0$^{3,8}$.0$^{4,7}$]nonane-$\underline{9}$-carboxamide (1), $C_{16}H_{14}BrNO$, $M_r = 316.2$, triclinic, $P\overline{1}$, $a = 10.129\ (2)$, $b = 12.007\ (2)$, $c = 11.676\ (2)$ Å, $\alpha = 99.44\ (1)$, $\beta = 88.27\ (2)$, $\gamma = 110.40\ (2)°$, $V = 1312.4\ (4)$ Å$^3$, $Z = 4$, $D_x = 1.600$ g cm$^{-3}$, $\lambda = 0.9252\ (1)$ Å, linear polarization 92%, $\mu = 9.11$ cm$^{-1}$, $F(000) = 640$, $T = 297$ K, $R = 0.026$ for 1920 reflections with $I > \sigma$.*

### 2.1. *Experimental*

A crystal of 0.024 × 0.23 × 0.30 mm (six faces) was glued to a glass fiber. Intensities of 2239 reflections (2090 independent) with $\theta < 25°$ were measured with synchrotron radiation 80 eV below the Br $K$ edge to minimize absorp-

---

* Pettersen (1966) reported $a = 10.09$, $b = 12.32$, $c = 11.64$ Å, $\alpha = 100.6$, $\beta = 88.3$, $\gamma = 114.1°$. This $b$, $\alpha$ and $\gamma$ are incorrect because of an error in transformation of the unit cell and should have been $b = 11.99$ Å, $\alpha = 99.6$, $\gamma = 110.3°$.

*Journal of Synchrotron Radiation*
ISSN 0909-0495 © 1995

tion; 14 were rejected as too strong, four for failure of repetitions to check, and 135 as too weak to measure. The Enraf–Nonius CAD-4 diffractometer (Phillips, Cerino & Hodgson, 1979) on Line 1-5 at SSRL [a bending-magnet line with an Si(111) double-crystal monochromator and no focusing, 50–100 mA ring current at 3 GeV] was used in a routine way with $\omega$-scan range 0.5° and scan time 30 s or less. The photon energy scale was based on 13.4821 keV for the $K$-edge maximum absorption of $NaBrO_3$. Absorption correction factors calculated by analytical integration ranged from 1.03 to 1.27. After normalization for beam intensity according to an ion chamber, 63 periodic measurements of 007 varied with $\sigma = 1.5\%$. Combination of equivalent pairs yielded 1920 unique reflections stronger than $\sigma(I)$. Starting with parameters from Pettersen (1966) (38 atoms with anisotropic thermal parameters, 28 H atoms isotropic, 455 parameters) least-squares refinement changed the bromine coordinates by less than 0.004 Å and the carbon coordinates by less than 0.05 Å. Bromine thermal parameters changed as much as 19%. Atomic scattering factors were taken from *International Tables for X-ray Crystallography* (1974) with dispersion corrections for all atoms calculated with the program of Cromer (1983). Atomic coordinates and equivalent isotropic thermal parameters are listed in Table 1.*

**Table 1**

Atomic coordinates and equivalent isotropic thermal parameters (Å$^2$).

| Atom | $x$ | $y$ | $z$ | $B_{eq}$† |
|---|---|---|---|---|
| Br(1) | 0.09592 (6) | 0.94510 (4) | 0.11480 (5) | 6.14 |
| Br(2) | 0.65576 (6) | 0.87126 (5) | 0.61752 (4) | 6.25 |
| C(1) | 0.0482 (4) | 0.7842 (3) | 0.1392 (3) | 3.86 |
| C(2) | 0.1225 (5) | 0.7555 (5) | 0.2184 (4) | 4.66 |
| C(3) | 0.0877 (4) | 0.6395 (4) | 0.2372 (4) | 4.30 |
| C(4) | −0.0215 (4) | 0.5498 (4) | 0.1750 (3) | 3.55 |
| C(5) | −0.0949 (4) | 0.5784 (4) | 0.0936 (3) | 4.02 |
| C(6) | −0.0595 (4) | 0.6956 (4) | 0.0767 (4) | 4.24 |
| C(7) | 0.0139 (4) | 0.3658 (3) | 0.2152 (3) | 3.75 |
| C(8) | −0.0662 (4) | 0.2389 (4) | 0.2364 (4) | 4.14 |
| C(9) | 0.0109 (5) | 0.1982 (4) | 0.3211 (4) | 5.07 |
| C(10) | −0.0948 (4) | 0.0831 (4) | 0.3579 (4) | 5.81 |
| C(11) | −0.2377 (5) | 0.1007 (4) | 0.3481 (3) | 4.94 |
| C(12) | −0.1985 (4) | 0.2216 (3) | 0.3068 (3) | 3.95 |
| C(13) | −0.1469 (4) | 0.2817 (4) | 0.4322 (3) | 4.11 |
| C(14) | −0.0036 (4) | 0.2646 (4) | 0.4417 (3) | 4.81 |
| C(15) | −0.0787 (4) | 0.1440 (4) | 0.4861 (4) | 5.53 |
| C(16) | −0.2216 (4) | 0.1612 (4) | 0.4768 (3) | 4.75 |
| N(1) | −0.0669 (5) | 0.4303 (4) | 0.1954 (3) | 4.23 |
| N(2) | 0.4395 (4) | 0.4370 (3) | 0.2380 (3) | 3.29 |
| O(1) | 0.1419 (3) | 0.4078 (2) | 0.2145 (2) | 4.96 |
| O(2) | 0.6330 (3) | 0.3904 (2) | 0.1908 (2) | 4.54 |
| C(21) | 0.5918 (4) | 0.7341 (3) | 0.4991 (3) | 3.83 |
| C(22) | 0.4560 (4) | 0.6561 (4) | 0.4992 (4) | 3.95 |
| C(23) | 0.4083 (4) | 0.5585 (4) | 0.4127 (3) | 3.54 |
| C(24) | 0.4950 (3) | 0.5362 (3) | 0.3261 (3) | 2.75 |
| C(25) | 0.6321 (4) | 0.6142 (3) | 0.3284 (4) | 3.60 |
| C(26) | 0.6803 (4) | 0.7131 (4) | 0.4144 (3) | 3.94 |
| C(27) | 0.5072 (4) | 0.3701 (3) | 0.1745 (3) | 3.09 |
| C(28) | 0.4212 (4) | 0.2719 (3) | 0.0811 (3) | 3.31 |
| C(29) | 0.4790 (3) | 0.1706 (3) | 0.0460 (3) | 3.60 |
| C(30) | 0.4000 (4) | 0.0962 (4) | −0.0672 (3) | 4.30 |
| C(31) | 0.3666 (4) | 0.1906 (3) | −0.1257 (3) | 4.07 |
| C(32) | 0.4304 (3) | 0.3081 (3) | −0.0384 (3) | 3.46 |
| C(33) | 0.5746 (4) | 0.3120 (3) | −0.0860 (3) | 3.36 |
| C(34) | 0.6080 (4) | 0.2182 (3) | −0.0278 (3) | 3.55 |
| C(35) | 0.5390 (4) | 0.1204 (3) | −0.1339 (3) | 4.10 |
| C(36) | 0.5056 (4) | 0.2138 (3) | −0.1914 (3) | 3.88 |

† $B_{eq} = (1/3)\sum_i\sum_j B_{ij}a_i^*a_j^*\mathbf{a}_i\cdot\mathbf{a}_j$.

There is good agreement of the corresponding bond distances and bond angles in the two independent molecules, but some differences of torsion angles are visible in the molecular conformations (Fig. 1). The dimensions of the homocubane cages conform closely to $mm2$ symmetry. Average values of C–C distances and angles that are equivalent in this symmetry are given in Table 2. The only deviations from this symmetry or differences of the cages in the two independent molecules that are larger than the estimated errors are displacements of C(8) and C(28) by 0.02 Å (in opposite directions with respect to the bonds to carbonyl). Crystal structures of some other derivatives of homocubane have been reported by Okaya (1969), Smits, Beurskens, Klunder & van der Loop (1986), Schäfer, Polborn & Szeimies (1988) and Watson, Kashyap, Marchand & Vidyasagar (1989).

**Table 2**

Distances (Å) and angles (°) in the homocubane cage, averaged according to $mm2$ symmetry.

| | | | |
|---|---|---|---|
| C(8)—C(9) | 1.518 (3) | C(9)—C(8)—C(12) | 95.6 (2) |
| C(9)—C(14) | 1.535 (2) | C(14)—C(9)—C(8) | 106.9 (1) |
| C(14)—C(13) | 1.535 (2) | C(14)—C(9)—C(10) | 87.3 (2) |
| C(14)—C(15) | 1.547 (2) | C(9)—C(14)—C(13) | 103.3 (1) |
| C(15)—C(16) | 1.536 (4) | C(9)—C(14)—C(15) | 91.6 (1) |
| | | C(13)—C(14)—C(15) | 89.8 (1) |
| | | C(14)—C(15)—C(10) | 86.5 (2) |
| | | C(14)—C(15)—C(16) | 90.2 (1) |

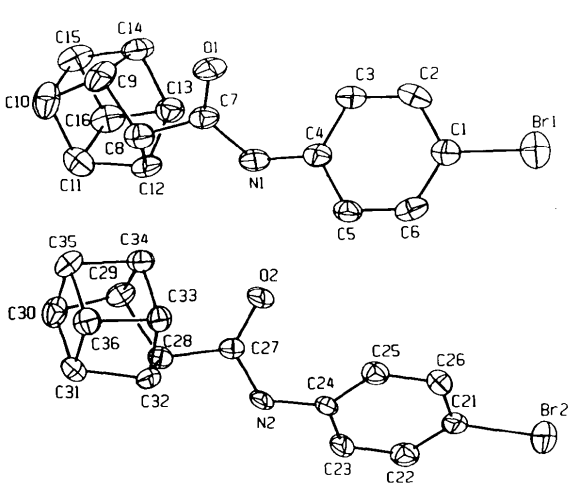

**Figure 1**

*ORTEP* (Johnson, 1976) views of the two independent molecules with numbering scheme and 30% probability thermal ellipsoids.

## 3. Absorption spectra

To guide the choice of wavelengths for the diffraction experiments we measured X-ray absorption spectra for

---

* Lists of structure factors, anisotropic thermal parameters, H-atom parameters, interatomic distances and bond angles have been deposited with the IUCr (Reference: MF0001). Copies may be obtained through The Managing Editor, International Union of Crystallography, 5 Abbey Square, Chester CH1 2HU, UK.

different directions of polarization in a crystal ($0.1 \times 0.1 \times 0.1$ mm in size) using the fluorescence-yield technique with a scintillation counter. It was expected (and later verified by the diffraction experiments) that Br in the two kinds of molecules would have atomic tensors that were equal (except for molecular orientation) and essentially uniaxial with the unique axis parallel with the direction of the respective bond [Br(1)–C(1) = 1.889 (4) Å, Br(2)–C(21) = 1.899 (3) Å]. The angle between these two directions is 56°. With these assumptions one can calculate the directions of the principal axes of the macroscopic tensor that controls the absorption spectra: the two bisectors of this vector angle and the direction perpendicular to both vectors. The perpendicular spectrum is like that of a single molecule. Spectra for the other two principal directions are linear combinations containing 22 or 78% of the parallel molecular spectrum [$\cos^2(56/2) = 0.78$].

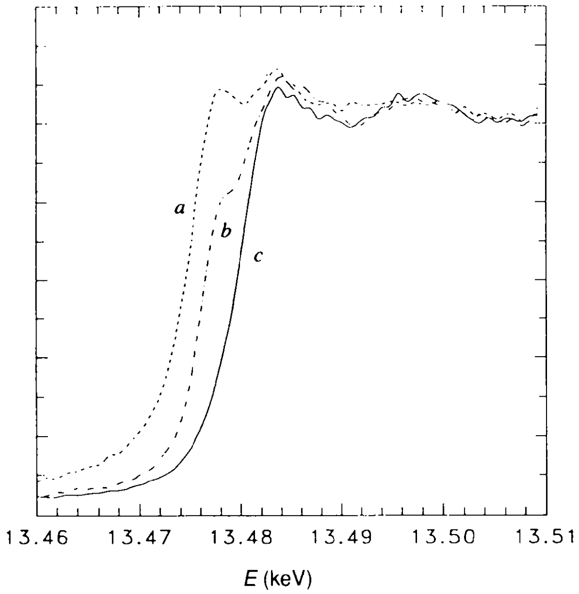

**Figure 2**
Single-crystal fluorescence-yield spectra with polarization in the direction of acute bisector of Br–C bond vectors (curve *a*), obtuse bisector (curve *b*), perpendicular to both bonds (curve *c*). Vertical scales are arbitrary and have been adjusted to equate edge jumps.

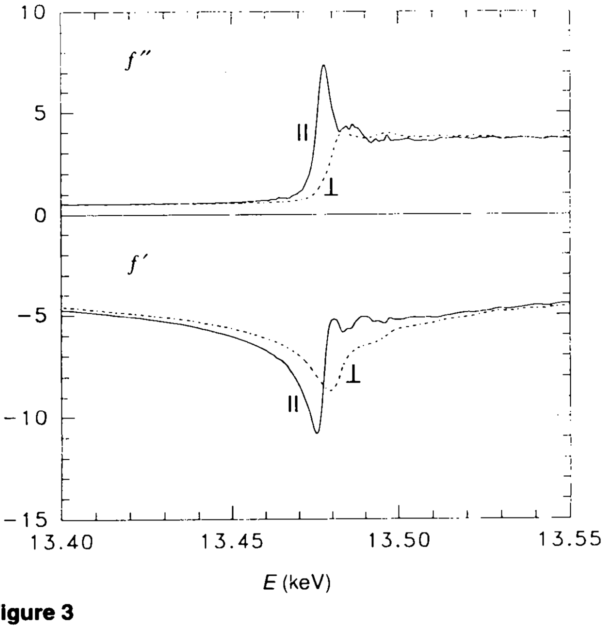

**Figure 3**
Principal values of $f''$ and $f'$ tensors calculated from spectra *b* and *c* of Fig. 2 as described in the text.

The spectra shown in Fig. 2 were measured with the polarization near the predicted principal axes of the macroscopic optical tensor. They display a parallel-polarized absorption at 13.478 keV as the transition of lowest energy. We assign it as excitation of a core electron to the $\sigma^*$ antibonding orbital that is associated with the Br–C single bond. This absorption is strongest for polarization in the direction most nearly parallel with the bond vectors (curve *a*), but the ratio of its intensity in curves *a* and *b* is less than the predicted 78/22. We attribute this discrepancy primarily to saturation of the spectra at high absorption because the crystal was too thick.

Principal values of $f''$ for Br, shown in Fig. 3, were calculated from curve *c* (Fig. 2) and from a linear combination $\mu(\sigma) = 4.54b - 3.54c$ that is a solution of the simultaneous equations $b = 0.22\mu(\sigma) + 0.78\mu(\pi)$ and $c = \mu(\pi)$. Also in Fig. 3 are values of $f'$ derived by Kramers–Kronig inversion of these $f''$ data by a difference method (Templeton & Templeton, 1988). Analogous calculations based on curves *a* and *c* indicated anisotropy that was qualitatively the same, but about half as much in magnitude.

## 4. Anisotropy of diffraction

When dispersion is treated in the dipole approximation, the complex scattering factor of an anisotropic atom is (in a Cartesian basis)

$$f(\mathbf{e},\mathbf{e}') = \sum_m e_m e'_m f_0 + \sum_{m,n} e_m e'_n S_{mn} \qquad (1)$$

for each of four combinations of linear polarization vectors $\mathbf{e}$ and $\mathbf{e}'$ of incident and scattered rays (Templeton & Templeton, 1982; Dmitrienko, 1983). Note that the Fourier transform of electron density that one uses to calculate the change of $f_0$ with Bragg angle takes account of retardation to all orders; in the dipole approximation $f_0$ is simply the number of electrons. Similarly, if the second-rank tensor $\mathbf{S}$ is made a function of Bragg angle it can include part of the effect of higher multipoles (that which is isotropic with respect to wavevectors). Values derived from diffraction measurements at a particular Bragg angle will contain this isotropic $\theta$-dependent part, but we expect it to be small in the experiment described here. Small anisotropic effects of higher multipoles have been observed in X-ray scattering (Finkelstein, Shen & Shastri, 1992; Templeton & Templeton, 1994), but we neglect them here.

Diffraction intensities for groups of reflections were measured at six energies near the absorption edge using the same crystal and techniques described in §2. Some details are listed in Table 3. The Bragg angle was limited to a narrow interval and each reflection was measured at azimuthal

**Table 3**
Diffraction experiments to measure tensors.

| $E$ (keV) | $\theta$ range (°) | $N$ | $R$ | $\mu_a$ (cm$^{-1}$) | $K$ |
|---|---|---|---|---|---|
| 13.4706 | 11–14 | 292 | 0.026 | 14 | –0.6 |
| 13.4730 | 11–14 | 628 | 0.030 | 21 | 0.4 |
| 13.4742 | 11–13 | 475 | 0.033 | 27 | 0.5 |
| 13.4754 | 11–14 | 643 | 0.033 | 38 | 1.1 |
| 13.4778 | 11–14 | 699 | 0.035 | 48 | 2.5 |
| 13.4802 | 11–13 | 345 | 0.032 | 58 | 1.0 |

$R = \sum|\Delta F|/\sum|F_o|$ for $N$ observations; $\mu_a$ and $K$ are parameters in equation (2).

**Table 4**
Tensor values from diffraction data.

| $E$ (keV) | $f_1'$ | $f_2'$ | $f_3'$ | $\sigma(f')$ | $f_1''$ | $f_2''$ | $f_3''$ | $\sigma(f'')$ |
|---|---|---|---|---|---|---|---|---|
| 13.4706 | –9.9 | –7.9 | –7.7 | 0.1 | 1.5* | – | – | 0.2 |
| | –9.6 | –7.8 | –7.6 | 0.1 | 0.8* | – | – | 0.3 |
| 13.4730 | –10.8 | –8.1 | –8.3 | 0.1 | 1.1 | 1.2 | 1.3 | 0.4 |
| | –11.1 | –8.2 | –8.2 | 0.1 | 2.2 | 1.5 | 0.9 | 0.3 |
| 13.4742 | –11.9 | –8.3 | –8.4 | 0.1 | 3.1 | 0.7 | 1.5 | 0.4 |
| | –12.1 | –8.2 | –8.4 | 0.1 | 2.3 | 0.5 | 0.8 | 0.4 |
| 13.4754 | –12.9 | –8.6 | –8.8 | 0.1 | 4.7 | 1.0 | 1.3 | 0.2 |
| | –13.2 | –8.7 | –8.7 | 0.1 | 4.1 | 0.9 | 0.8 | 0.2 |
| 13.4778 | –11.6 | –9.2 | –9.3 | 0.2 | 9.0 | 1.1 | 1.7 | 0.3 |
| | –12.2 | –8.9 | –9.2 | 0.2 | 8.6 | 0.7 | 1.6 | 0.3 |
| 13.4802 | –6.4 | –9.8 | –10.0 | 0.2 | 6.0 | 2.6 | 2.9 | 0.4 |
| | –6.5 | –10.3 | –9.7 | 0.2 | 5.7 | 2.8 | 2.6 | 0.4 |

Values for Br(1) are listed in the first line, for Br(2) in the second line at each photon energy; $f_1$ is parallel with the bond vector, $f_2$ is parallel with the plane of the benzene ring and perpendicular to the bond, $f_3$ is perpendicular to the ring plane. * Isotropic $f''$ refined at this wavelength.

settings –45, 0 and 45° in order to permit wide ranges of directions for the various vectors within the available time. Correction factors for absorption in this pleochroic crystal were calculated repeatedly by analytical integration using a separate value of $\mu$ for each intensity datum; $\mu$ was calculated by the equation (Templeton & Templeton, 1991)

$$\mu = \mu_a(1 + K\mathbf{s}^T\mathbf{M}\mathbf{s}), \tag{2}$$

where the average absorption coefficient $\mu_a$ was estimated from the absorption spectra, **s** is the unit polarization vector perpendicular to the plane of scattering, and $K$ was adjusted by trial and error to achieve the best agreement in least-squares calculations of the scattering tensors. Correction factors ranged from 1.02 to 6.84 in the most anisotropic case. We chose a Cartesian basis with axes in the directions **a**, **c*** × **a** and **c*** for the vector and tensor calculations. In this basis the anisotropy matrix calculated from the atomic coordinates (assuming equal uniaxial tensors for Br atoms) is

$$\mathbf{M} = \begin{pmatrix} -0.3254 & 0.0219 & 0.0368 \\ 0.0219 & 0.4334 & 0.0931 \\ 0.0368 & 0.0931 & -0.1080 \end{pmatrix}. \tag{3}$$

This correction for absorption is a good approximation for the *ss* term which dominates the intensity for most of the reflections.

A full-matrix least-squares minimization of $\sum(|F_o| - |F_c|)^2/\sigma^2(F_o)$ was used to determine a scale factor and 24 tensor parameters (real and imaginary elements of symmetric 3 × 3 matrices for two independent Br atoms) from each data set. All atomic coordinates and displacement parameters were held fixed at the values found in the structure refinement. The integrated intensity was corrected for absorption, Lorentz factor and scale (but not for polarization) to give $|F_o|^2$, and $|F_c|^2 = |F_{ss}|^2 + |F_{sp}|^2$. Here $p$ refers to the polarization component in the plane of scattering. We omitted *pp* and *ps* terms which are small because the incident radiation contains only 4% $p$ polarization. The *sp* term also is small, but is significant for some of the weak reflections.

At one energy $f''$ was too small for a valid determination of its anisotropy, and it was constrained to be isotropic. At the next energy the $f''$ tensor is too nearly isotropic for the directions of its principal axes to be meaningful. The other tensors are uniaxial within $3\sigma$ and have their unique axes nearly parallel with the bond; the average angle of deviation for the $12\,f'$ tensors is 4° (maximum 11°) and that for $8\,f''$ tensors is 8° (maximum 21°), or 5° (maximum 7°) if those at 13.4742 keV are excluded. These deviations are probably less than the errors. According to the local symmetry at the Br atom, principal axes should be along the bond and parallel or perpendicular to the benzene ring. Tensor values for each atom for these three directions are listed in Table 4. Within the statistical accuracy the tensors are the same for the two molecules and for the two directions perpendicular to each bond. The averages of these values are plotted in Fig. 4.

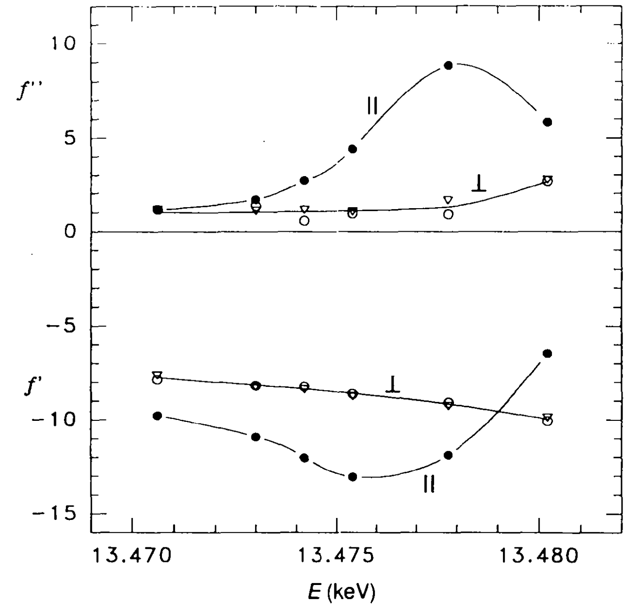

**Figure 4**
Average principal values of the tensors for the two independent Br atoms, derived from diffraction data. Solid circles, polarization parallel with bond; open circles, in benzene plane; triangles, out of plane.

## 5. Discussion

This experiment adds another item to the growing list of chemical states which exhibit strong X-ray dichroism that arises from resonant absorption to valence-band levels. The anisotropy of scattering, as much as 4.3 for $f'$ and 7.5 for $f''$, is not exceptional for a $K$ edge. Maximum values measured for Br in the bromate ion were about 4.6 and 6.6 (Templeton & Templeton, 1985*a*) and for divalent Se were 5.9 and 6.9 (Templeton & Templeton, 1988). We do not have tensors for the $Br_2$ molecule, but the appearance of the spectra (Kincaid & Eisenberger, 1975; Heald & Stern, 1978) suggests that they will be equally anisotropic. Because the radiation bandwidth (*ca* 2 eV) in our experiment is comparable to the Br $K$ level width (2.5 eV; Krause & Oliver, 1979) we expect that even larger values would be found with better resolution. This anisotropy is large enough to be useful and to require attention, or at least caution, in experiments where multiple wavelengths are used to manipulate scattering factors. The anisotropy of $f''$ is largely concentrated in a rather narrow spectral interval and perhaps can be avoided by working not too close to the edge. That of $f'$ is more extended in wavelength and more difficult to avoid. The effects on diffraction intensities are reduced if the incident radiation is unpolarized, but they are not eliminated.

The reduction of $R$ to 0.026 in the crystal structure refinement and in one of the tensor experiments indicates the precision that was achieved at wavelengths away from an edge. The larger values (up to 0.035) for other data sets can be explained by the extreme sensitivity of $f$ to slight shifts of wavelengths near the resonance or by defects in the absorption correction.

Absorption corrections tend to be the limiting factor in the accuracy of structure factors measured in this kind of diffraction experiment, as indeed they often are in routine crystal structure work. It is fortunate that the design of the present experiment made the tensor parameters not very sensitive to this error. The absorption correction used here improved the agreement of observed and calculated structure factors, compared with earlier calculations using the method described by Templeton & Templeton (1991), but had little effect on the tensor parameters. In the most anisotropic case (13.4778 keV) it reduced $R$ from 0.050 to 0.035. With a conventional isotropic correction $R$ was 0.076 for this data set.

We thank the many staff members of Stanford Synchrotron Radiation Laboratory whose assistance made this work possible. We are particularly indebted to Dr Michael Soltis. This research was supported in its initial stages by the National Science Foundation under Grant CHE-8821318. It was performed in part at SSRL, which is operated by the Department of Energy, Office of Basic Energy Sciences. The SSRL Biotechnology Program is supported by the NIH, Biomedical Resource Technology Program, Division of Research Resources. Further support is provided by the Department of Energy, Office of Health and Environmental Research. Also used were facilities of the Lawrence Berkeley Laboratory, supported by the Director, Office of Energy Research, Office of Basic Energy Sciences, Chemical Sciences Division of the US Department of Energy under Contract No. DE-AC03-76SF00098.

## References

Cromer, D. T. (1983). *J. Appl. Cryst.* **16**, 437.

Dauben, W. D. & Whalen, D. L. (1966). *Tetrahedron Lett.* pp. 3743–3750.

Dmitrienko, V. E. (1983). *Acta Cryst.* A**39**, 29–35.

Fanchon, E. & Hendrickson, W. A. (1990). *Acta Cryst.* A**46**, 809–820.

Finkelstein, K. D., Shen, Q. & Shastri, S. (1992). *Phys. Rev. Lett.* **69**, 1612–1615.

Heald, S. M. & Stern, E. A. (1978). *Phys. Rev. B*, **17**, 4069–4081.

Hendrickson, W. A. (1991). *Science*, **254**, 51–58.

*International Tables for X-ray Crystallography* (1974). Vol. IV, pp. 72–80. Birmingham: Kynoch Press. (Present distributor Kluwer Academic Publishers, Dordrecht.)

Johnson, C. K. (1976). *ORTEP*II. Report ORNL-5138. Oak Ridge National Laboratory, Tennessee, USA.

Kincaid, B. M. & Eisenberger, P. (1975). *Phys. Rev. Lett.* **34**, 1361–1364.

Kirfel, A. & Petcov, A. (1991). *Z. Kristallogr.* **195**, 1–15.

Kirfel, A. & Petcov, A. (1992). *Acta Cryst.* A**48**, 247–259.

Krause, M. O. & Oliver, J. H. (1979). *J. Phys. Chem. Ref. Data*, **8**, 329–338.

Okaya, Y. (1969). *Acta Cryst.* B**25**, 1882–1889.

Pettersen, R. C. (1966). PhD Thesis, Univ. of California, Berkeley, USA.

Phillips, J. C., Cerino, J. A. & Hodgson, K. O. (1979). *J. Appl. Cryst.* **12**, 592–600.

Schäfer, J., Polborn, K. & Szeimies, G. (1988). *Chem. Ber.* **121**, 2263–2265.

Smits, J. M. M., Beurskens, P. T., Klunder, A. J. H. & van der Loop, E. A. R. M. (1986). *J. Crystallogr. Spectrosc. Res.* **16**, 657–663.

Templeton, D. H. & Templeton, L. K. (1982). *Acta Cryst.* A**38**, 62–67.

Templeton, D. H. & Templeton, L. K. (1985*a*). *Acta Cryst.* A**41**, 133–142.

Templeton, D. H. & Templeton, L. K. (1985*b*). *Acta Cryst.* A**41**, 365–371.

Templeton, D. H. & Templeton, L. K. (1987). *Acta Cryst.* A**43**, 573–574.

Templeton, D. H. & Templeton, L. K. (1991). *Acta Cryst.* A**47**, 414–420.

Templeton, D. H. & Templeton, L. K. (1992). *Acta Cryst.* A**48**, 746–751.

Templeton, D. H. & Templeton, L. K. (1994). *Phys. Rev. B*, A**49**, 14850–14853.

Templeton, L. K. & Templeton, D. H. (1988). *Acta Cryst.* A**44**, 1045–1051.

Watson, W. H., Kashyap, R. P., Marchand, A. P. & Vidyasagar, V. (1989). *Acta Cryst.* C**45**, 2010–2012.